

Sequential tunneling and spin degeneracy of zero-dimensional states

M. R. Deshpande,^{*} J. W. Sleight,[†] M. A. Reed, and R. G. Wheeler

Departments of Physics, Applied Physics, and Electrical Engineering Yale University, P.O. Box 208284, New Haven, Connecticut 06520
(Received 14 September 1999)

The effects of the spin degeneracy of single, zero-dimensional, localized, donor impurity states are investigated. We report a nontrivial effect on the zero-magnetic-field current-voltage [$I(V)$] characteristics of a localized state resulting from its spin degeneracy. We detect a deviation from the expected Fermi function thermal broadening of the observed current step in the $I(V)$ characteristics. We quantitatively model this deviation in a sequential tunneling picture in terms of a new phenomenological parameter, the occupancy of the localized state (p). The spin degeneracy of the state is lifted in a magnetic field (Zeeman splitting) causing the current step to split. The two fragments of the split current step are observed to have different magnitudes. An investigation of this effect also enables the measurement of p as reported earlier [Phys. Rev. Lett. **76**, 1328 (1996)]. We compare the two methods of determining the occupancy (p) and find a good agreement between them. Both these methods also enable us to determine the electron tunneling rates across each of the two potential barriers of the device independently. We also identify certain features in the $I(V)$ characteristics at higher bias that have different thermal and magnetic-field properties than most other regular features. We attribute these to double occupancy of the electrons in the localized states when the barrier for that is overcome at higher bias. The phenomenological theory developed in this paper explains these observations quite accurately.

I. INTRODUCTION

The experimental realization of granular electronic systems, such as low-dimensional semiconductor and ultrasmall metallic systems, has focused attention on the basic physical properties of discrete electronic systems. Especially intriguing are the semiconductor quantum dot¹⁻⁵ and the physically similar localized impurity state tunneling systems.⁶⁻¹⁴ The latter consists of donor impurity atoms in the quantum-well regions of resonant tunneling diodes. This system provides a unique laboratory for the investigation of single, isolated, zero-dimensional, localized states. Investigation of the basic spin properties of such states has become significant also due to recent interests in quantum computing. Spins of single atoms embedded in a semiconductor have been proposed for use as q -bits for computation.^{15,16} There has also been a lot of activity in the field of spin transport.¹⁷ The donor atom, in our experimental system, at low temperatures and in a magnetic field acts as a very effective spin filter.

In this paper we investigate the effects of the spin degeneracy of the localized donor impurity states on the device current-voltage [$I(V)$] characteristics. We observe that the degeneracy does not simply contribute a factor of two, but exhibits itself in a nontrivial manner even in the zero-magnetic-field $I(V)$ characteristics. We model this effect in a sequential tunneling picture. Electron-electron repulsion and Coulomb charging energies act as barriers to double occupation of the degenerate spin states. Thus even though the spin degeneracy implies availability of two states, they cannot contribute to the full extent for tunneling. We introduce a single phenomenological parameter, the occupancy of the impurity state p , which characterizes how much the impurity state is occupied. This enables us to quantitatively explain the zero-magnetic-field $I(V)$ characteristics. The same parameter p also explains the peculiarities observed in the $I(V)$

characteristics in a magnetic field. The experimental determination of p enables us to independently determine the electron tunneling rates through each of the two potential barriers of the device. The electron-electron repulsion and Coulomb energy barrier can be overcome by applying a higher bias. We observe features in the $I(V)$ characteristics at high bias that we attribute to the simultaneous occupation of two electrons in the impurity state.¹⁸ These features have different thermal and magnetic-field properties, which distinguish them from regular features.

Isolated donor impurities in the quantum-well regions of large area resonant tunneling diodes form localized (~ 100 Å) hydrogenic states bound to the quantum eigenstates. Figure 1 illustrates the band diagram of a device used in this study with one impurity state in the well schematically noted. Under an applied bias the current exhibits a steplike increase, as the impurity state aligns with the emitter Fermi level. In general, there may be multiple impurities giving rise

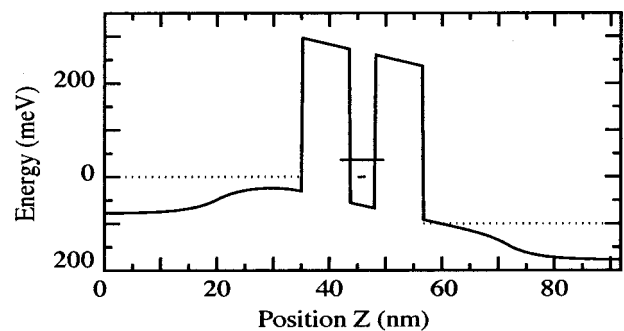


FIG. 1. Model conduction-band diagram of a resonant tunneling diode device at an applied bias of 100 mV. The simulated quantum eigenstate (long line) and a schematically represented localized impurity state (short line) are shown in the well. The dotted lines represent the Fermi levels in the leads.

to multiple, overlapping steps in the current-voltage characteristics. An appropriately dilute, unintentional doping concentration allows the measurement of a single impurity state. At very low temperatures the Fermi distribution function is an abrupt step function and hence the $I(V)$ characteristics show current steps that are sharp. As the temperature of the device is increased, the emitter Fermi level broadens. The current steps also broaden, but we observe that a Fermi function fit to the broadening^{4,5,11,12} of the current steps is inadequate (Fig. 5). The experimentally measured plateau current is observed to saturate at a lower value than the current predicted by the Fermi fit. Similarly a peculiarity is observed in the $I(V)$ characteristics with applied magnetic field (Fig. 8). The magnetic field lifts the spin degeneracy of the state (Zeeman splitting) and causes the current step to split.^{11,12,19} The two fragments of the Zeeman split current step are observed *not* to have the same magnitude even though there is no spin polarization in the emitter. We propose a phenomenological model that explains both the effects. This understanding and our model enables us to independently determine the electron tunneling rates through the two potential barriers in a sequential tunneling picture.^{4,20} The thermal broadening and the magnetotunneling are two independent measurements of the tunneling rates and are in good agreement with each other.

In Sec. II we present our phenomenological model of tunneling through a localized impurity state. In Sec. III we give the details of the device growth and characterization. In Sec. IV B we investigate the thermal broadening of the features in the $I(V)$ characteristics and in Sec. IV C we discuss the results from the magnetic-field measurements. In Sec. IV D we identify a small number of steps in the $I(V)$ characteristics that show substantially different thermal broadening and no splitting in a magnetic field. These steps are attributed to two electrons occupying the impurity state at the same time.

II. THEORY

A. Theory: Zero-magnetic-field tunneling

The tunneling of electrons through localized, zero-dimensional (0D) states in the quantum-well region of a double barrier, single quantum-well device may be modeled in the sequential tunneling picture. In this picture the tunneling process is viewed as two separate processes, as schematically represented in Fig. 2. The first process is tunneling from the emitter to the localized state and the second process is tunneling from the localized state to the collector. In order to derive an expression for current, we define T_{em} and T_{cl} to be the electron tunneling rates for tunneling across the emitter and the collector barriers, respectively. These rates depend upon both the applied bias and the available density of states in the respective contact electrodes to which the localized state can couple. We define p to be the occupancy of the electron in the localized state, which is essentially the probability of the state being occupied by an electron.

Let us first consider the case of a single, nondegenerate localized state. In steady electron flow condition, the rate of electrons tunneling into the localized state is the same as the rate of electrons tunneling out. The rate of inflow from the emitter is equal to T_{em} times the occupancy of states with energy E in the emitter [which is simply the Fermi function,

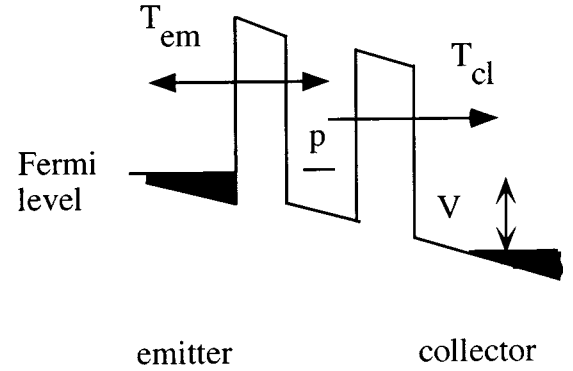


FIG. 2. Schematic representation of electrons tunneling from the emitter to the collector through a single localized state in the well. T_{em} and T_{cl} denote the electron tunneling rates for tunneling across the emitter and the collector barriers, respectively, and p denotes the occupancy of the electron in the localized state. V denotes the applied bias across the device.

$f(E)$] times the probability of the localized state being unoccupied [which is $(1-p)$]. Once the electron is in the localized state it can either tunnel back to the emitter at a rate $p[1-f(E)]T_{em}$ or it can tunnel out into the collector at a rate pT_{cl} . We can see from the band alignment in Fig. 2 that the occupancy of the collector states is not of concern as the Fermi level in the collector is much below the localized energy state. Hence we have

$$f(E)[1-p]T_{em} = p[1-f(E)]T_{em} + pT_{cl}, \quad (1)$$

which gives

$$p = f(E) \frac{T_{em}}{T_{em} + T_{cl}}, \quad (2)$$

which is just the partial tunneling rate. The tunneling current through a single, localized state under such circumstances is given by

$$\Delta I = epT_{cl} = ef(E) \frac{T_{em}T_{cl}}{T_{em} + T_{cl}}. \quad (3)$$

Therefore the current resulting from electrons tunneling through single, *nondegenerate*, localized states is exactly proportional to the Fermi distribution function $f(E)$ and it is not possible to experimentally determine both T_{em} and T_{cl} independently.

So far we have assumed that the localized impurity state is nondegenerate. However, the ground state of the impurity potential consists of not one but two states due to spin degeneracy. If the two channels due to the two spin states are independent then one expects the tunneling probability and the current to double and the occupancy to become $2p$. However, the two tunneling channels are not independent of each other. Two electrons cannot occupy the two available spin states at the same time due to the large electron-electron repulsion and Coulomb charging energy required for the second electron to simultaneously occupy the second spin state of the localized state in the well. For this system, the single-electron Coulomb charging energy ($U_c = e^2/2C$, where C is the effective capacitance of the double barrier diode) is very

large compared to the thermal energy ($kT \leq 250 \mu\text{eV}$) or the Zeeman energy ($\leq 150 \mu\text{eV}$). The effective capacitance of the device can be estimated as $C = (\epsilon_0 k \pi r_0^2)(d_t^{-1} + d_b^{-1})$, where k is the dielectric constant, d_t and d_b are the top and bottom barrier thicknesses, and r_0 ($\approx 100 \text{ \AA}$) is the Bohr radius of hydrogenic impurities in GaAs. This gives $U_C \approx 9 \text{ meV}$. Hence for small bias changes ($\leq 1 \text{ mV}$) we can assume that the simultaneous occupation of two electrons in the two available spin states cannot take place.

If p is the occupancy if there is only one tunneling channel then $2p$ is the occupancy if there are two independent tunneling channels and p^2 is the probability of occupying the two channels simultaneously. Thus the occupancy when either one of the two states but not both can be occupied is $(2p - p^2)$. Hence the current through such a two-state system can be written as

$$\Delta I = e(2-p)pT_{cl} = \left(2 - f(E) \frac{T_{em}}{T_{em} + T_{cl}}\right) e f(E) \frac{T_{em} T_{cl}}{T_{em} + T_{cl}}. \quad (4)$$

If p is small compared to 1 then the current through the twofold degenerate system [Eq. (4)] is just twice that of the current through a single-state system [Eq. (3)] and is proportional to the Fermi function, $f(E)$. However, if p is large, then the current would not be directly proportional to the Fermi function.

This is a simple, phenomenological theory to understand tunneling through a two-state spin system in terms of a single parameter p . A more accurate theory will have to take into account many-body effects, total spin, and other issues in a perturbative analysis as has been done by Akera for a similar system involving quantum dots.²¹ Our theory, and the equation for current [Eq. (4)], is, however, a good approximation and it provides a useful physical insight into the tunneling system.

B. Theory: Magnetotunneling

In a magnetic field the spin degeneracy of the localized state is lifted due to Zeeman splitting and the two spin states have different energies. In high magnetic fields (when the Zeeman splitting energy is relatively large) and at low temperatures (when the Fermi level is sharp), we can adjust the bias near a given localized state to have the following two conditions as shown schematically in Fig. 3. At lower bias, V_1 , only the lower-energy spin state is below the emitter Fermi level and hence only one channel is active for conduction. In this case the current is given by

$$I_1 = p e T_{cl}. \quad (5)$$

At a higher bias, V_2 , the higher-energy spin state is also below the Fermi level and thus both channels are active for conduction. The current in this case (by arguments similar to the ones in Sec. II A) is given by

$$I_2 = p' e T_{cl} = e(2-p)p T_{cl}, \quad (6)$$

where $p' = (2p - p^2)$ is the occupancy for having either the lower or the higher-energy spin state but not both of them occupied simultaneously. If p is small compared to 2 then the current through the two spin states [Eq. (6)] is just twice that

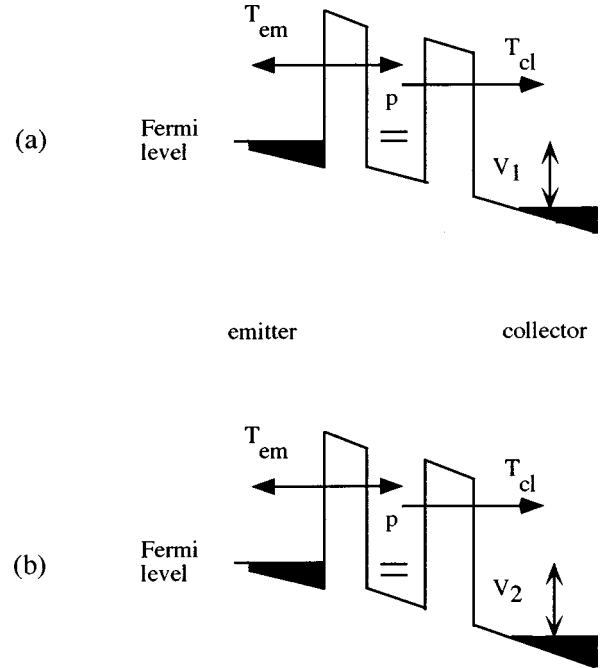


FIG. 3. Schematic representation of electrons tunneling through a two-state spin system in a magnetic field. (a) At lower bias, V_1 , only the lower-energy spin state is below the emitter Fermi level and hence available for tunneling. (b) At higher bias, V_2 , both spin states are below the emitter Fermi level and electrons can tunnel through either.

of current through a single state [Eq. (5)]. But if p is not negligible, then the current magnitudes of the two fragments of the Zeeman split current step [I_1 and $(I_2 - I_1)$] would not be the same.

In Eqs. (5) and (6) we have assumed that the Fermi function $f(E)$ is a sharp step function which is a good assumption at low temperatures (less than 0.1 K) when the thermal energy is smaller than the spin splitting energy. We have also assumed that the tunneling rates are the same at the two different biases V_1 and V_2 , which is a good assumption if the bias difference ($V_2 - V_1$) is much smaller than the barrier potential. In our case the experimentally determined spin splitting energy ($\Delta E \leq 150 \mu\text{eV}$) is much smaller than the barrier potential energy ($\approx 300 \text{ meV}$). We also assume that the emitter electrons are not spin polarized since the emitter Fermi energy ($\sim 40 \text{ meV}$) is much larger than the spin splitting energy even at 10 T.

III. SAMPLE DESIGN

The nominally symmetric resonant tunneling heterostructures are grown by molecular beam epitaxy (MBE) on a Si-doped GaAs (100) substrate.²² The epitaxial layers consist of a $1.8 \times 10^{18} \text{ cm}^{-3}$ Si-doped GaAs contact, a 150- \AA undoped GaAs spacer layer, an undoped $\text{Al}_{0.27}\text{Ga}_{0.73}\text{As}$ bottom barrier of width w , a 44- \AA undoped GaAs quantum well, an undoped $\text{Al}_{0.27}\text{Ga}_{0.73}\text{As}$ top barrier of nominally the same width w , a 150- \AA undoped GaAs spacer layer, and a $1.8 \times 10^{18} \text{ cm}^{-3}$ Si-doped GaAs top contact. Square mesas with lateral dimensions from 2 to 64 μm are fabricated using standard photolithography techniques. In this paper we report investigations of two specific devices only. One has w

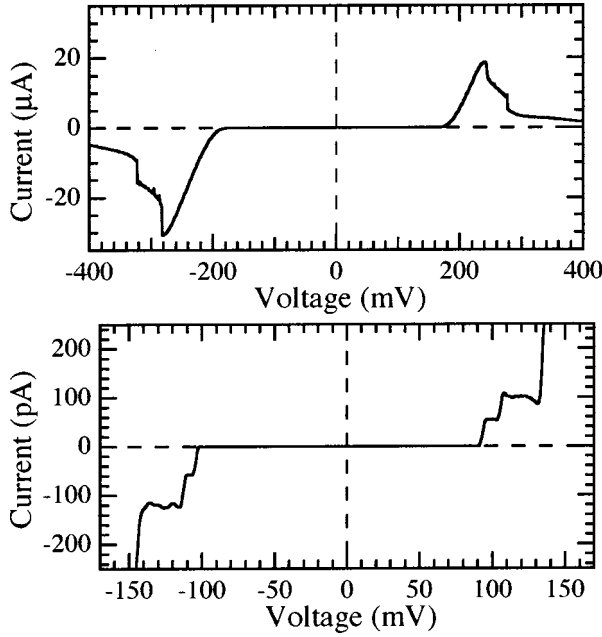


FIG. 4. $I(V)$ characteristics (zero magnetic field) at 1.4 K of the 85-Å barrier resonant tunneling diode device showing the main resonance peaks (top). The magnified prethreshold region shows two steplike structures due to two isolated impurities (bottom).

=85 Å and a lateral dimension of 8 μm and the other has $w = 65$ Å and a lateral dimension of 16 μm. Two terminal dc $I(V)$ characteristics are measured using a low-noise amplifier. The variable temperature measurements are done in a Janis liquid-helium cryostat and the high magnetic-field measurements are done in an Oxford dilution refrigerator with a mixing chamber base temperature (T_{mix}) of 35 mK.

IV. OBSERVATIONS

A. Tunneling through impurities

Figure 4 shows the $I(V)$ characteristics of a resonant tunneling diode device at 1.4 K, showing the main quantum-well resonance peaks (top). Magnification of the current in the prethreshold region (bottom) shows two sharp current steps for both forward- and reverse-bias directions. This step structure is observed to be sample specific, but for a given sample it is exactly reproducible from one voltage sweep to another and independent of the voltage sweep direction. The steps are reproduced even after repeated thermal cycling of the sample, except for slight threshold voltage shifts. Similar features have been observed and reported previously,^{6,7,9} and the various current steps are attributed to tunneling through the bound states of separate, localized, 0D impurity states in the quantum well.

B. Zero-magnetic field variable temperature measurements

In this section we investigate the temperature dependence of the current steps in the $I(V)$ characteristics in zero magnetic field. As discussed in the theory section [Sec. II and expressed in Eq. (3)], the magnitude of the current step in tunneling through a *single* electronic state is proportional to f , the Fermi distribution function. The sharpness of the current plateau edge is thus expected to decrease as the tempera-

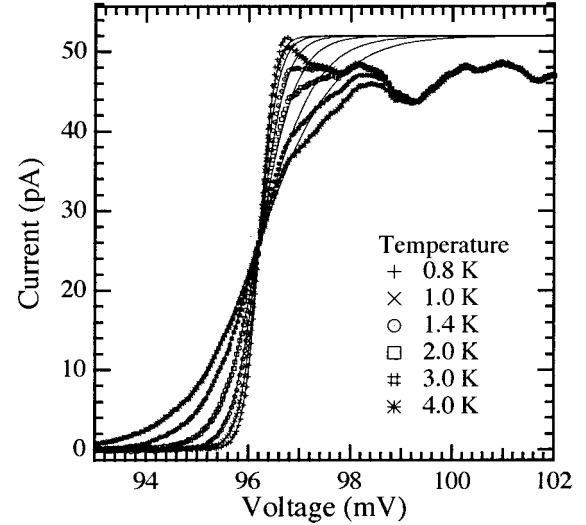


FIG. 5. $I(V)$ characteristics of the first current step edge in forward bias of the 85-Å barrier device at different temperatures showing the Fermi-level broadening and the Fermi fit [Eq. (7)] to these $I(V)$ traces. The fits are done for biases less than the threshold ($V \leq V_{th}$) and then extrapolated to voltages greater than the threshold. The experimentally measured plateau current is seen to be less than the theoretically expected, extrapolated plateau current.

ture increases, due to the broadening of the emitter Fermi distribution. We can express the current [Eq. (3)] as

$$I(V, T) = 2I_{th}f(V - V_{th}, T) = \frac{2I_{th}}{1 + \exp[\alpha e(V_{th} - V)/kT]}, \quad (7)$$

where e is the electron charge, k is the Boltzmann's constant, and V_{th} and I_{th} are the threshold voltage and current values at the observed common intersection point of the various $I(V)$ curves at different temperatures. α is the voltage to energy conversion factor. It is the ratio of the voltage drop between the quantum well and the emitter to the total voltage across the device.^{4,5,23} Since the localized state has two barriers of nominally the same width on either side, we expect α to be approximately equal to half. Due to the asymmetric band bending we also expect α to be slightly smaller than half as more voltage gets dropped across the collector barrier than the emitter barrier. Note that when $V = V_{th}$, $f(0, T) = 1/2$, and $I = I_{th}$ irrespective of the temperature. The only free parameter is thus α , and is determined to be equal to 0.48 from a fit (Fig. 5) of the above function to the $I(V)$ traces at zero magnetic field. The fits are done only for the region $V \leq V_{th}$ because of the presence of an oscillatory structure on the current plateaus. We refer to this structure as the “fine structure” and it is attributed to the fluctuations in the local density of states in the contact electrodes.^{5,9} This fine structure has been investigated in detail by Schmidt *et al.*^{13,14} Figure 5 also shows the extrapolation of the fits of Eq. (7) to the data to voltages greater than the threshold ($V \geq V_{th}$). The experimental plateau current value is observed to be smaller than that predicted by the extrapolated Fermi fit. We attribute this deviation from the Fermi behavior to the spin degeneracy of the localized state and Coulomb charging effects as discussed in Sec. II. This shows that the spin de-

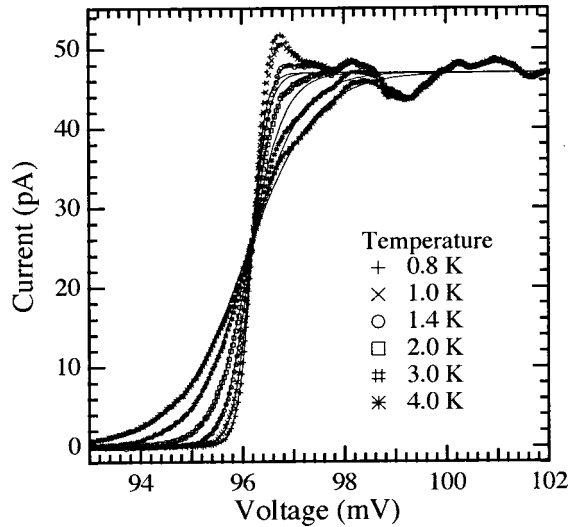


FIG. 6. $I(V)$ characteristics of the first current step edge in forward bias of the 85-Å barrier device at different temperatures and the corrected fits [Eq. (8)] to these $I(V)$ traces. The fits are done for biases less than the threshold ($V \leq V_{th}$) and then extrapolated to voltages greater than the threshold.

generacy indeed affects the $I(V)$ characteristics in a non-trivial manner even for zero magnetic field.

The current in the case of tunneling through two degenerate states [Eq. (4)] can be expressed as

$$\Delta I = A p_0 f(E) [2 - p_0 f(E)], \quad (8)$$

where A is a constant and $p_0 = T_{em}/(T_{em} + T_{cl})$ is the occupancy of the electron in either one of the two localized degenerate states when $f(E) = 1$ [Eq. (2)]. p_0 depends upon the relative tunneling rates of the two potential barriers. Equation (8) can be fit to the data (Fig. 6). Once again the fits are done only for bias voltages $V \leq V_{th}$ because of the presence of the “fine structure” on the current plateaus for $V \geq V_{th}$. V_{th} is obtained from the common intersection point of the curves at different temperatures. A and p_0 are obtained from the measured values of the plateau current ($I_{plateau}$) and the threshold current I_{th} in the following way. When $V \geq V_{th}$ then $f(E) = 1$ and

$$\Delta I = I_{plateau} = A p_0 (2 - p_0). \quad (9)$$

When $V = V_{th}$ then $f(E) = 1/2$ and

$$\Delta I = I_{th} = A (p_0/2) (2 - p_0/2). \quad (10)$$

Solving these two equations simultaneously from the measured values of $I_{plateau}$ and I_{th} we determine A and p_0 . From the data shown in Fig. 6, $A = 81.4$ pA and $p_0 = 0.35$. Thus once again the only free parameter in the fitting equation [Eq. (8)] is α which is accurately determined to be 0.50. An extrapolation of these fits to bias voltages $V \geq V_{th}$, however, now accurately determines the current plateau value as shown in Fig. 6, where as previously the fit of the Fermi function alone predicted a higher plateau current value.

It is also possible to determine the occupancy for the localized states in reverse bias. For the same device in reverse bias we obtain $p_0 = 0.57$ and $\alpha = 0.42$. This difference in for-

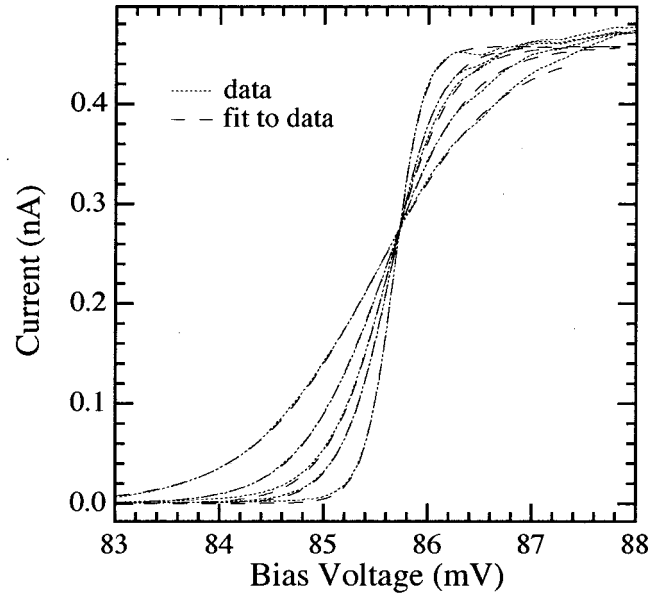


FIG. 7. $I(V)$ characteristics of the first current step edge in forward bias of the 65-Å barrier thickness device at different temperatures and the corrected fits [Eq. (8)] to these $I(V)$ traces. The fits are done over the entire bias range spanning the step. The sharpest step is at 0.7 K and the successively broader steps are at 1.2, 1.5, 2, and 3 K.

ward and reverse bias is attributed to a slight asymmetry in the growth of the device and will be discussed more later.

The importance of this corrected fit becomes even more apparent while investigating the thermal broadening of current steps on which the fine structure is not very prominent. In such cases the fit can be carried out over the entire range of the data unlike the earlier case where it was restricted to $V \leq V_{th}$. This is shown in Fig. 7 for the 65-Å barrier thickness device in forward bias. From the fit we obtain $p_0 = 0.57$, $A = 0.56$ nA, and $\alpha = 0.42$ for this particular step. Note that only using a Fermi fit [Eq. (7)] to the data of Fig. 7 would be very inaccurate. The ratio of the current at the threshold V_{th} , the common intersection point of all the curves, and the current on the plateau is $I_{th}/I_{plateau} = 0.275$ nA/0.458 nA = 0.6. This is much larger than 0.5 that is expected in case of a perfect Fermi function dependence.

1. Electron tunneling rates

From the experimental values of A and p_0 one can determine the electron tunneling rates T_{em} and T_{cl} . $p_0 = T_{em}/(T_{em} + T_{cl})$ and $A = e T_{cl}$. Thus for the first current step in forward bias of the 85-Å barrier thickness device (Fig. 6), $T_{cl} = 510$ MHz and $T_{em} = 270$ MHz. Similarly for the first current step in forward bias of the 65-Å barrier device (Fig. 7), $T_{cl} = 3.6$ GHz and $T_{em} = 4.7$ GHz. It is not possible to theoretically estimate T_{em} and T_{cl} accurately and separately because the exact nature of the impurity and its location is not known. However, their order of magnitude can be estimated. The tunnel rates for the 65-Å barrier device are observed to be an order of magnitude higher than those for the 85-Å barrier device. This is consistent with the order of magnitude higher current step magnitude. It is also consistent with a numerical evaluation of the quantum-well

eigenstate lifetime which predicts the correct order of magnitude for the current step magnitudes for devices with different barrier thicknesses.²³ This estimation was done using the simulation program, BANDPROF, developed by Frenslay.²²

Significant insight into the tunneling process and the device details can be obtained by analyzing the relative values of T_{em} , T_{cl} , and p for forward- and reverse-bias orientations. For the 85-Å barrier device we have $p=0.35$ for forward bias and $p=0.57$ for reverse bias. A less than 0.5 value for p , as in forward bias, indicates that the collector (downstream) barrier tunnel rate (T_{cl}) is higher than the emitter (upstream) barrier tunnel rate (T_{em}) causing a depletion from the well. A high p value (greater than 0.5), as in reverse bias, indicates that the electron tunneling rate through the collector (downstream) barrier (T_{cl}) is lower than that through the emitter (upstream) barrier (T_{em}) causing an accumulation in the well. A higher p value for reverse bias (as compared to forward bias) suggests an asymmetry in the heterostructure growth with one barrier being slightly thicker than other barrier. The biasing of the device is such that in forward bias the top barrier is the emitter barrier while in reverse bias the top barrier is the collector barrier. This implies that the top barrier is slightly thicker than the bottom barrier. This is consistent with the difference in the measured α values (α in forward bias is higher than α in reverse bias), observed asymmetry in the $I(V)$ characteristics for this sample (the main resonance peak voltage and peak current values are higher for reverse bias as compared to forward bias (Fig. 4) and is in agreement with previous characterization.²²

Similar measurements of the tunneling rates can also be obtained from the magnetic-field studies as discussed in the next section. However, those measurements require low temperature (less than 300 mK) and high magnetic fields. The method described here requires only relatively moderate (greater than 1 K) variable temperature measurements.

C. Low-temperature magnetotunneling measurements

Now we will investigate the effects of the spin degeneracy of the localized states on the $I(V)$ characteristics in a magnetic field. In this section we will confine the discussion to magnetic fields oriented parallel to the current flow (perpendicular to the quantum well). Figure 8 shows an expanded view of the current step in both forward- and reverse-bias orientation, with and without a magnetic field, when the sample is in a dilution fridge with the base temperature of the fridge (T_{mix}) at 35 mK. For zero field, the ground state of the impurity is spin degenerate leading to a single current step. Upon lifting of the degeneracy at finite fields, a splitting of the current step is observed.

Figure 8 shows that the two fragments of the spin-split step at 11 T do *not* have the same current magnitudes [$(I_2 - I_1) \neq I_1$], where I_1 and I_2 mark the current values as shown. I_1 gives the current of the first fragment while I_2 is the net current of both fragments of the split step edge. This difference is more prominent in reverse bias.

We understand this peculiarity in terms of the finite occupancy of the impurity state and the Coulomb charging energy according to the model discussed in Sec. II. We refer once again to Eqs. (5) and (6) that model the current magnitude through the spin-split current step. In the extreme limits

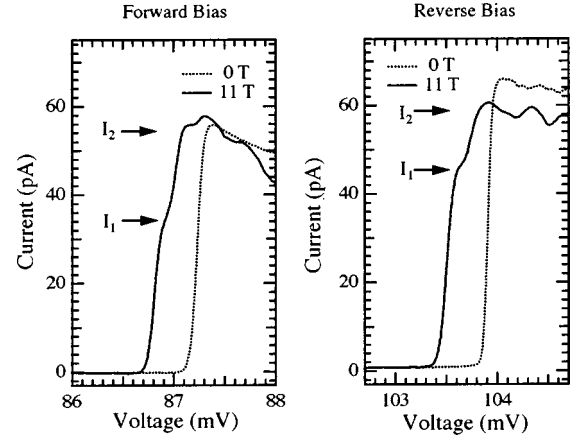


FIG. 8. $I(V)$ characteristics at $T_{mix}=35$ mK of the first current step edge of the 85-Å barrier device in forward bias (left) and reverse bias (right) at 0 T (dotted line) and 11 T (solid line). The magnetic field is oriented parallel to the current direction. I_1 and I_2 mark the current values at 11 T as shown. I_1 gives the current of the first fragment while I_2 is the net current of both fragments of the split step edge. The curves have some arbitrary voltage offset for clarity.

these equations indicate that for $T_{cl} \gg T_{em}$, $p \approx 0$ and $I_2 \approx 2I_1$ while for $T_{cl} \ll T_{em}$, $p \approx 1$, and $I_2 \approx I_1$. This qualitatively explains the behavior observed in Fig. 8. To get a quantitative understanding, we solve Eqs. (5) and (6), using the experimentally measured I_1 and I_2 , to determine p and also the tunneling rates T_{em} and T_{cl} .

From the data shown in Fig. 8 at 11 T (the field parallel to the current), we get $p=0.3$ for forward bias and $p=0.6$ for reverse bias. These agree quite well with the determination of occupancy from the zero-field thermal broadening measurements (Sec. IV B). From Eqs. (5) and (6) we can also obtain the absolute magnitude of the electron tunneling rates through the two potential barriers and investigate their dependence upon the magnetic field. Figure 9 shows the tunneling rates and the probability of occupation p as a function of the magnetic field parallel to the current in forward bias. The oscillations observed in the tunneling rate and in p (Fig. 9) are due to the fine structure on the current plateaus and its systematic shift in a magnetic field.^{5,9,13,14} Nevertheless, it is possible to extrapolate them to zero field and compare to those obtained from variable temperature measurements in Sec. IV B. The two measurements are observed to be in good agreement.

D. Double occupancy of the localized state

So far in this paper we have ignored double occupancy of the impurity localized state by electrons of both the up and the down spin at the same time. In this section we would like to explore the possibility of such an occurrence.

In Sec. II A we mentioned that there are two effects that try to prevent simultaneous occupation of two electrons in the localized state in the well. One is Coulomb energy and the other is electron-electron repulsion energy. Coulomb energy depends upon the resonant tunneling diode barrier thicknesses and the lateral size of the localized state and is estimated to be of the order of 9 meV (Sec. II A). The electron-electron repulsion energy is more difficult to esti-

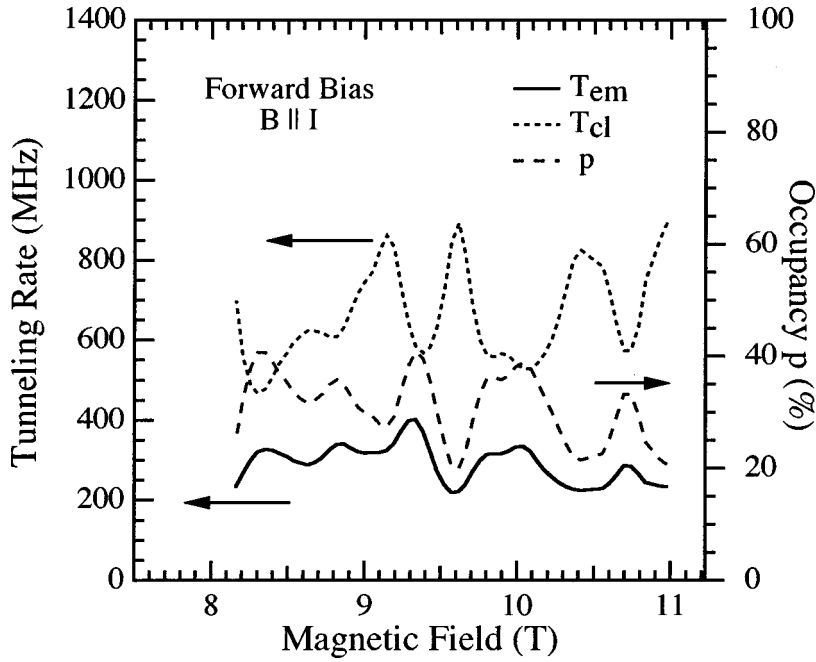


FIG. 9. Tunneling rates T_{em} and T_{cl} and the occupancy p as a function of the magnetic-field strength parallel to current for the 85-Å barrier device in forward-bias orientation.

mate as it requires knowledge of the exact nature of the localized impurity and its charge state. The simplest case is if the impurity is hydrogenic in nature. In that case it has a single positive charge when unoccupied by electrons (H^+), it is neutral when it is occupied by one electron (H), and it is like a negative hydrogenic ion (H^-) when doubly occupied. The binding energies of hydrogenic atoms (H) in a GaAs quantum well are about 10 to 15 meV.²⁵ Hence we estimate the electron-electron repulsion energy for two electrons simultaneously occupying the localized impurity state to be of the order of a few meV too. Thus the total-energy barrier for double occupancy ($\Delta U_{double\ occupancy}$) is on the order of 20 meV.

This barrier for double occupancy can be overcome by applying higher bias. An additional bias ($\Delta V_{double\ occupancy}$) of the order of 20 meV/ $\alpha e \sim 40$ mV is required beyond the bias corresponding to the first occurrence of the step in the $I(V)$ characteristics. At such a bias, an additional channel for the electrons to tunnel opens up as simultaneous occupation of the impurity becomes possible. We expect this to exhibit itself as an additional step in the current-voltage characteristics. At higher biases one also has other independent impurity states available for tunneling. Due to the inherent nature of this experimental system, being that of a multi-impurity system, it is difficult to identify the steps in the $I(V)$ characteristics. However, we expect the steps due to double occupancy to have some special properties, which would distinguish them from other regular steps.

From the theory Sec. II A, we know that the tunneling current through a two-state degenerate system allowing tunneling through either of the two states but not both simultaneously is given by [Eq. (4)]

$$\Delta I(V) = e(2p - p^2)T_{cl}, \quad (11)$$

where $(2p - p^2)$ is the occupancy when either one of the two states but not both can be occupied. If the barrier for double occupancy is overcome then we expect to see a step in the $I(V)$ characteristics of magnitude,

$$\begin{aligned} \Delta I(V + \Delta V_{double\ occupancy}) &= e(p^2)T_{cl} \\ &= e \left(f(E) \frac{T_{em}}{T_{em} + T_{cl}} \right)^2 T_{cl}, \end{aligned} \quad (12)$$

where (p^2) is the contribution that was not allowed at the lower bias.

The tunneling rates (T_{em} and T_{cl}) in Eq. (12) are different from those in the previous equation (11) because tunnel rates depend upon bias, as the bias modulates the tunneling barriers. Hence direct comparison of the current step magnitudes to identify steps related to double occupancy is not possible. However, Eq. (12) predicts that the current step due to double occupancy would be proportional to the square of the Fermi distribution function and hence would have different thermal broadening than regular current steps. One also expects that this step would not split in a magnetic field like other steps because it is attributed to that fraction of the current through the two-spin state system where both the spins are simultaneously occupied.

Observations of such current steps in the $I(V)$ characteristics are presented in Figs. 10. The magnetic field in this figure is oriented perpendicular to the current flow direction unlike the case for the data presented in Sec. IV C. In forward bias (Fig. 10) steps 3 and 7 are seen to *not* split in the magnetic field. Step 3 may be too close in bias to step 4 for an unambiguous interpretation; however, step 7 is clearly separate from step 8. Similarly we observe step 4 in reverse bias (figure not shown) to *not* split while all other steps split in the magnetic field.

We attribute steps 3 and 7 in forward bias to be the double-occupancy-related steps associated with the same impurities that cause steps 1 and 2, respectively, in forward bias (Fig. 4). All other steps are observed to split, and are attributed to different independent impurities. We get the bias differences $(V_{step3} - V_{step1}) = (137 - 96) = 41$ mV; $(V_{step7} - V_{step2}) = (145 - 109) = 36$ mV. These differences compare

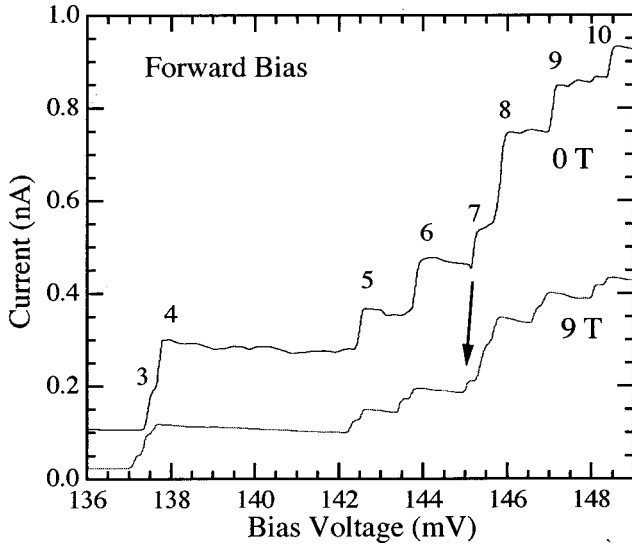


FIG. 10. Current-voltage characteristics of the 85-Å barrier device in forward bias at 0 T and 9 T (at a mixing chamber base temperature of 35 mK). The magnetic field is oriented perpendicular to the current flow direction. Different steps in the $I(V)$ characteristics are numbered at 0 T. There are two steps at biases less than 136 mV that are not shown here (see Fig. 4). Steps marked 3 and 7 are seen to *not* split in the magnetic field; all other steps split.

quite well with the order of magnitude estimation of the double-occupancy energy ($\Delta V_{\text{double occupancy}} \sim 40$ mV) thus giving credibility to our assignment.

Another important and interesting observation is that the current magnitudes of all the steps attributed to double occupancy are substantially more suppressed in the magnetic field than the regular steps. Note that the magnetic field in this case is oriented perpendicular to the current flow direction. In this orientation the current through the localized state gets suppressed as the electron tunneling rate decreases in the magnetic field due to reduced overlap of the wave functions.^{12,24} In a magnetic field the probability of occupation (p) decreases. For regular steps the current is proportional to $(2p-p^2)$ and is linear in p for small p . For the double-occupancy steps the current is proportional to p^2 (quadratic in p). Hence the current suppression is expected to be much more for the double-occupancy steps. This observation corroborates our theory and the attribution of the specified steps to double occupancy.

Another way in which a current step attributable to double occupancy can be distinguished is by investigating its thermal broadening at zero magnetic field. Figure 11 shows the thermal broadening of step 4 in reverse bias at different temperatures from 0.15 to 1.0 K. A fit of the square of the Fermi function to that data is also shown. Equation (12) predicts that current steps attributed to double occupancy would be proportional to p^2 and hence to $(f(E))^2$. The fit shown in Fig. 11 is in excellent agreement with the theory. Note that the threshold current (current at the common intersection point of the data at different temperatures) in Fig. 11 is less than half the total step current. This clearly indicates that a simple Fermi function [Eq. (3)] or the corrected function used in Sec. IV B to understand the regular current steps [Eq. (4)] are not suitable for this step and they would not be able to describe the data for any choice of the fitting parameters.

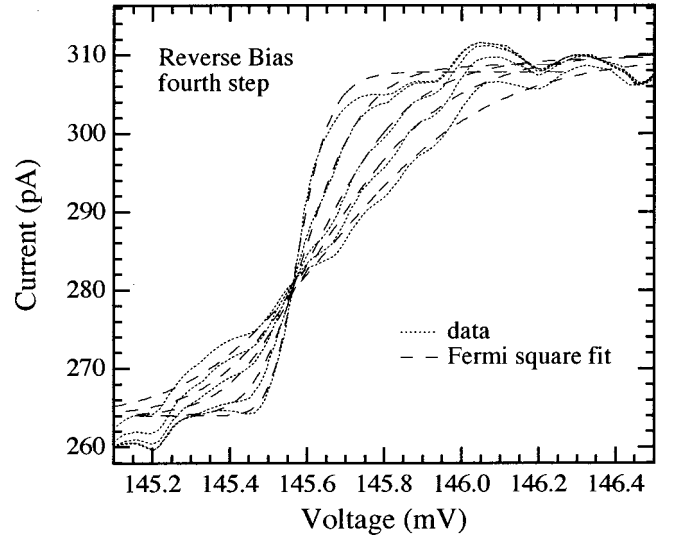


FIG. 11. Current-voltage characteristics of the fourth step in reverse bias of the 85-Å barrier device at different temperatures and fit to the data of the square of the Fermi distribution function $[(f(E))^2]$. The data are at temperatures 0.15, 0.3, 0.5, 0.7, and 1.0 K.

This fit thus confirms the theory that the current step is due to double occupancy of electrons in the localized state.

V. CONCLUSIONS

We have investigated the effects of spin degeneracy on electronic transport through single, zero-dimensional, localized impurity states. In Sec. IV B we reported *non-Fermi* thermal broadening of the current steps in the $I(V)$ characteristics. This effect is modeled by introducing a new phenomenological parameter p , the occupancy of the localized, impurity state. The corrected equation fits the $I(V)$ characteristics quite accurately and p is determined from the fits.

In Sec. IV C the finite occupancy of the impurity state p is invoked to understand the peculiarities of the tunneling $I(V)$ characteristics through the impurity in a magnetic field. From these measurements the occupancy p is determined as a function of the magnetic field and then extrapolated to zero field. For the first current step in forward bias of the 85-Å barrier device we determine the occupancy $p=0.3$ from magnetic-field measurements. This is in good agreement with the measured value of $p=0.35$ from the variable temperature investigation. In reverse bias for the same device we determine $p=0.6$ and $p=0.57$, respectively, from the two measurements.

A single parameter p , the occupancy of the impurity state, explains the non-Fermi thermal broadening and also the peculiar splitting in a magnetic field of the current step in the $I(V)$ characteristics. These two independent and consistent measurements support the correctness of our model. From the measured occupancy and the plateau current magnitudes we determine the electron tunneling rates through the emitter and the collector barriers independently. The determination of the tunneling rates from the variable temperature investigation alone is significant since it does not require high magnetic fields or very low temperatures as are required for the magnetotunneling measurements.

Finally in Sec. IV D we discussed the possibilities of two electrons occupying a localized state at the same time. This becomes possible at high bias when the charging and the electron-electron repulsion energies are overcome. We identified steps in the $I(V)$ characteristics at higher bias that show substantially different magnetic field and thermal properties compared to the regular current steps. We attribute these current steps to double occupancy of the localized state. The phenomenological theory developed in this paper describes these observations satisfactorily.

The peculiarities in the $I(V)$ characteristics, as reported in this paper, arise due to the fundamental properties of spin degeneracy of localized states and electron-electron repul-

sion. We expect to see similar effects in other related experimental systems such as quantum dots and molecular electronic systems.

ACKNOWLEDGMENTS

We thank T. Senthil, Sharad Ramanathan, and Professor D. E. Prober for many useful discussions, R. J. Matyi for device growth, C. L. Fernando and Professor W. R. Frensley for help with the modeling, and A. Mittal for experimental assistance. This work is supported by NSF Grant No. DMR-9112497 and No. 9216121.

*Present address: Motorola Labs., 7700 S. River Parkway, M/D ML 34 Tempe, AZ 85284.

Email: Mandar.Deshpande@Motorola.com

†Present Address: IBM Semiconductor Research and Development Center, 1580 Route 52, B/630 Zip E40, Hopewell Junction, New York 12533.

¹M. A. Reed, J. N. Randall, R. J. Aggarwal, R. J. Matyi, T. M. Moore, and A. E. Wetsel, Phys. Rev. Lett. **60**, 535 (1988).

²S. Tarucha, Y. Hirayama, T. Saku, and T. Kimura, Phys. Rev. B **41**, 5459 (1990).

³M. Teoword, L. Martin-Moreno, V. J. Law, M. J. Kelly, R. Newbury, M. Pepper, D. A. Ritchie, J. E. F. Frost, and G. A. C. Jones, Phys. Rev. B **46**, 3948 (1992).

⁴B. Su, V. J. Goldman, and J. E. Cunningham, Phys. Rev. B **46**, 7644 (1992).

⁵J. W. Sleight, E. S. Hornbeck, M. R. Deshpande, R. G. Wheeler, M. A. Reed, R. C. Bowen, W. R. Frensley, J. N. Randall, and R. J. Matyi, Phys. Rev. B **53**, 15 727 (1996).

⁶M. W. Dellow, P. H. Beton, C. J. G. M. Langerak, T. J. Foster, P. C. Main, L. Eaves, M. Henini, S. P. Beaumont, and C. D. W. Wilkinson, Phys. Rev. Lett. **68**, 1754 (1992).

⁷J. W. Sakai, P. C. Main, P. H. Beton, N. La Scala, Jr., A. K. Geim, L. Eaves, and M. Henini, Appl. Phys. Lett. **64**, 2563 (1994).

⁸A. K. Geim, P. C. Main, N. La Scala, Jr., L. Eaves, T. J. Foster, P. H. Beton, J. W. Sakai, F. W. Sheard, M. Henini, G. Hill, and M. A. Pate, Phys. Rev. Lett. **72**, 2061 (1994).

⁹M. R. Deshpande, J. L. Huber, N. H. Dekker, P. Kozodoy, J. W. Sleight, M. A. Reed, C. L. Fernando, W. R. Frensley, R. J. Matyi, and Y. C. Kao, in *22nd International Conference on the Physics of Semiconductors*, edited by D. J. Lockwood (World Scientific, Singapore, 1995), p. 1899.

¹⁰J. W. Sakai, N. La Scala, Jr., P. C. Main, P. H. Beton, T. J. Foster, A. K. Geim, L. Eaves, M. Henini, G. Hill, and M. A. Pate, Solid-State Electron. **37**, 965 (1994).

¹¹M. R. Deshpande, J. W. Sleight, M. A. Reed, R. G. Wheeler, and R. J. Matyi, Phys. Rev. Lett. **76**, 1328 (1996).

¹²M. R. Deshpande, J. W. Sleight, M. A. Reed, R. G. Wheeler, and R. J. Matyi, Superlattices Microstruct. **20**, 513 (1996).

¹³T. Schmidt, R. J. Haug, V. I. Falko, K. v. Klitzing, A. Foerster, and H. Lueth, Europhys. Lett. **36**, 61 (1996).

¹⁴T. Schmidt, R. J. Haug, V. I. Falko, K. v. Klitzing, A. Forster, and H. Luth, Phys. Rev. Lett. **78**, 1540 (1997).

¹⁵B. Kane, Nature (London) **393**, 133 (1998).

¹⁶R. Vrijen, E. Yablonovitch, K. Wang, H. W. Jiang, A. Baladin, V. Roychowdhury, T. Mor, and D. DiVincenzo, quant-ph/9905096 (1999) (unpublished).

¹⁷S. K. Upadhyay, R. N. Louie, and R. A. Buhrman, Appl. Phys. Lett. **74**, 3881 (1999).

¹⁸J. G. S. Lok, A. K. Geim, J. C. Maan, I. Marmoros, F. M. Peeters, N. Mori, L. Eaves, T. J. Foster, P. C. Main, J. W. Sakai, and M. Henini, Phys. Rev. B **53**, 9554 (1996).

¹⁹A. S. G. Thornton, T. Ihn, P. C. Main, L. Eaves, and M. Henini, Appl. Phys. Lett. **73**, 354 (1998).

²⁰We assume sequential tunneling because the barriers are thick (85 Å). S. Luryi, Appl. Phys. Lett. **47**, 490 (1985).

²¹H. Akera, Phys. Rev. B **60**, 10 683 (1999).

²²M. A. Reed, W. R. Frensley, W. M. Duncan, R. J. Matyi, and A. C. Seabaugh, Appl. Phys. Lett. **54**, 1256 (1989).

²³M. R. Deshpande, Ph.D. thesis, Yale University, 1998.

²⁴J. W. Sakai, T. M. Fromhold, P. H. Beton, L. Eaves, M. Henini, P. C. Main, F. W. Sheard, and G. Hill, Phys. Rev. B **48**, 5664 (1993).

²⁵G. Bastard, Phys. Rev. B **24**, 4714 (1981).